Journal of Zhejiang University SCIENCE A
ISSN 1673-565X (Print); ISSN 1862-1775 (Online)
www.zju.edu.cn/jzus; www.springerlink.com
E-mail: jzus@zju.edu.cn

Optimization of total harmonic current distortion and torque pulsation reduction in high-power induction motors using genetic algorithms

Arash SAYYAH[1], Mitra AFLAKI[‡2], Alireza REZAZADEH[3]

([1]*Department of Electrical and Computer Engineering, University of Illinois at Urbana-Champaign, Urbana, IL 61801, USA*)

([2]*Graduate School of Management and Economics, Sharif University of Technology, Tehran, Iran*)

([3]*Department of Electrical and Computer Engineering, Shahid Beheshti University, Tehran, Iran*)

E-mail: sayyah1@uiuc.edu; mitra.aflaki@gmail.com; alireza.rezazade@gmail.com

Received Jan. 17, 2008; revision accepted June 1, 2008; CrossCheck deposited Nov. 10, 2008

Abstract: This paper presents a powerful application of genetic algorithm (GA) for the minimization of the total harmonic current distortion (THCD) in high-power induction motors fed by voltage source inverters, based on an approximate harmonic model. That is, having defined a desired fundamental output voltage, optimal pulse patterns (switching angles) are determined to produce the fundamental output voltage while minimizing the THCD. The complete results for the two cases of three and five switching instants in the first quarter period of pulse width modulation (PWM) waveform are presented. Presence of harmonics in the stator excitation leads to a pulsing-torque component. Considering the fact that if the pulsing-torques are at low frequencies, they can cause troublesome speed fluctuations, shaft fatigue, and unsatisfactory performance in the feedback control system, the 5th, 7th, 11th, and 13th current harmonics (in the case of five switching angles) are constrained at some pre-specified values, to mitigate the detrimental effects of low-frequency harmonics. At the same time, the THCD is optimized while the required fundamental output voltage is maintained.

Key words: Induction motor, Genetic algorithm (GA), Optimization, Pulse width modulation (PWM), Torque pulsation, Total harmonic current distortion (THCD)
doi:10.1631/jzus.A0820055 **Document code:** A **CLC number:** TM346

INTRODUCTION

Among all power converters used in industry, the pulse width modulated (PWM) inverters have the most widespread applications such as uninterruptible power supply (UPS), phase controlled rectifier, and adjustable speed servo drives due to their capabilities of controlling the output voltage and frequency simultaneously, and generating output waveform with low harmonic distortion. At low to medium power levels, simple modulation methods are desirable for limiting system complexity and cost. Additionally, the relatively low power rating permits the use of power switches which can operate at high switching frequencies, so that satisfactory waveforms can be generated without having to optimize each individual switching instant. Nevertheless, at high power levels, to limit switching losses, power semiconductor devices (e.g., gate turn-off, GTO) that can only operate at low switching frequencies (typically several hundred Hz) are utilized. In this case, direct optimization of the waveform based on specification of an optimal value for each switching instant seems indispensable. This optimization can be achieved via various approaches. The two predominant methods in choosing the switching instants are "harmonic elimination and minimization of the total harmonic distortion" (Chiasson *et al.*, 2002). The former method aims at

‡ Corresponding author

complete elimination of some low-order harmonic components from the inverter output and is the more widely used and straightforward of the two techniques. In contrast, in the latter method the waveform is defined in a way to minimize the harmonic losses of electrical loads fed by the inverter. In the harmonic elimination method, switching patterns can be determined by solving some systems of nonlinear and transcendental equations (Sun and Grotstollen, 1994; Mohan *et al.*, 1995). These transcendental equations are solved using iterative numerical techniques, where the initially provided approximate solutions must be sufficiently close to the exact solutions to ensure the convergence of the solutions, and this is the most difficult task associated with these methods (Sun, 1995). Some attempts have been made to simplify harmonic elimination equations by applying Walsh functions (Asumadu and Hoft, 1989; Park *et al.*, 1990). It was believed that the system of transcendental nonlinear harmonic elimination equations resulting from Fourier analysis of PWM waveform could be replaced by a system of linear algebraic equations when Walsh analysis is applied. However, it has been illustrated that the Walsh functions approach is neither theoretically nor practically applicable (Sun, 1995). In some other studies (Chiasson *et al.*, 2004), the complete solutions to the harmonic elimination problem have been presented using the theory of resultants from elimination theory (Kailath, 1980; Cox *et al.*, 1996; Chen, 1999). These expressions are difficult and time consuming to derive. An increase in the number of switching angles can exacerbate the problem due to its call for exorbitant calculations. Ozpineci *et al.*(2005) have improved their preceding works from computational view point by application of the genetic algorithm (GA) optimization technique for determining the switching angles for a cascaded multilevel inverter, which eliminates specified higher order harmonics while maintaining the required fundamental voltage. More comparisons between the suggested methods in the harmonic elimination approach have been made in (Sayyah *et al.*, 2006b).

In present work, we have defined total harmonic current distortion (THCD) as the objective function to be optimized in lieu of concentrating on specific harmonics considering some drawbacks of the harmonic elimination approach. One disadvantage of the harmonic elimination approach originates from the fact that as the total energy of harmonics in a PWM waveform is constant, elimination of lower-order harmonics considerably boosts the remaining ones (Bose, 1986). Since the harmonic losses in a machine are determined by the ripple currents, a performance index related to undesirable effects of the harmonics should be defined to minimize instead of focusing on individual harmonics.

In this study we have concentrated our efforts on optimizing THCD in high power induction motors, based on an approximate harmonic model of the motor operating in steady-state conditions. GA is preferred to the numerical methods used in (Sun, 1995), where the initially provided approximate solution has a pivotal role in the convergence of the algorithm, or to the inefficient and time-consuming complete scanning method. The main distinguishing feature of the proposed method lies in the fact that due to its stochastic nature, it can cope with limitations of aforementioned approaches with more likelihood of finding the global optimum. Presence of harmonics in the stator excitation leads to a pulsing-torque component. Low-order current harmonics (in the case of five switching angles) are constrained at some pre-specified values to mitigate the detrimental effects of low-frequency harmonics. Existence of constraints significantly affects the performance of every optimization algorithm. GA appears as an appropriate technique for constraint handling. From the practical perspective, this method (minimization of total harmonic distortion) was considered and implemented in (Rezazadeh *et al.*, 2006) for a high-power synchronous machine, which exhibits a more complicated objective function, and experimental results corroborate the developed technique.

PROBLEM STATEMENT

As high power applications are concerned, it is advantageous to impose the switching frequency to be synchronized with the fundamental frequency (Holtz, 1992). This assumption ensures that, in steady-state conditions, the modulated output waveform remains unchanged for certain fundamental periods. In addition, to ensure the nonappearance of even-order harmonics, each waveform is assumed to

be quarter-period symmetrical and half-period inversely symmetrical. A two-level normalized PWM waveform is shown in Fig.1.

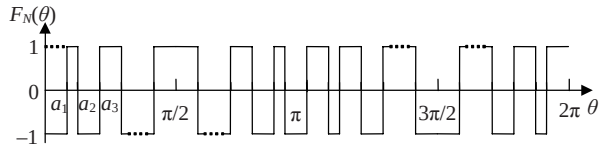

Fig.1 A line-to-neutral PWM structure

Waveform representation

A PWM waveform is uniquely determined if its structure has been specified and the N switching instants in the first quarter period have been defined. Obviously, these angles must satisfy the basic constraint:

$$0 < \alpha_1 < \alpha_2 < ... < \alpha_{N-1} < \alpha_N \le \pi/2. \tag{1}$$

For each waveform, we use an (N+1)-dimensional vector $\boldsymbol{h}$=[h_0, h_1, h_2, …, h_N] to represent its initial level at θ=0 and the variation of levels at all N switch instants (Sun *et al.*, 1996). The Fourier series expansion of the output voltage waveform of the PWM inverter as illustrated in Fig.1 can be determined as

$$f(\theta) = \sum_{k=1,3,5,...} V_k \sin(k\theta), \tag{2}$$

where

$$\begin{aligned} V_k &= \frac{4}{\pi}\int_0^{\pi/2} f(\theta)\sin(k\theta) \\ &= \frac{4}{k\pi}\left(h_0 + \sum_{i=1}^{N} h_i \cos(k\alpha_i)\right) \\ &= \frac{4}{k\pi}\sum_{i=0}^{N} h_i \cos(k\alpha_i), \end{aligned} \tag{3}$$

in which α_0=0.

Approximate harmonic model of the motor

The harmonic equivalent circuit and its approximation of an induction motor operating in steady-state conditions are illustrated in Fig.2 (Murphy and Turnbull, 1988). The approximation of the equivalent circuit is deduced regarding that inductive reactance increases linearly with frequency, while the stator and rotor resistances are almost constant. The skin effect which causes the rotor resistance to increase with frequency has been neglected. Since s_k is approximate unit, circuit resistance is negligible in comparison with reactance at the harmonic frequency. In addition, the magnetizing inductance L_m is much larger than the rotor leakage inductance L_2 and may be omitted (Sun, 1995). Hence, the motor impedance presented to the kth-order harmonic input voltage is $k\omega_1(L_1+L_2)$ and the kth-order current harmonic would be

$$I_k = \frac{V_k}{k\omega_1(L_1+L_2)} \propto \frac{V_k}{k}. \tag{4}$$

Based on the derived result, we can define the objective function of this optimization as

$$\sigma_i = \sqrt{\sum\nolimits_{k\in S_h} (V_k/k)^2}, \tag{5}$$

where S_h is the set of harmonics in consideration. For single- and three-phase inverters, S_h=$S_{1\phi}$={3, 5, ..., 2l+1, ...} and S_h=$S_{3\phi}$={5, 7, ..., 6l−1, 6l+1, ...}, respectively.

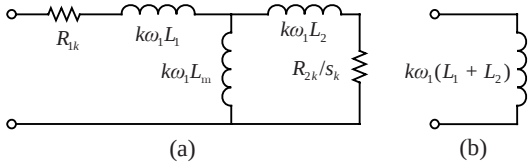

Fig.2 Equivalent circuit of an induction motor operating in steady-state conditions (k>1). (a) The kth-order harmonic equivalent circuit; (b) Approximation of (a)

It should be noted that minimization of the objective function σ_i corresponds to the minimization of motor harmonic current distortion (the subscript i is intended to indicate the current fact), and also to the minimization of harmonic copper losses of the motor windings.

Closed-form expressions of objective function

Closed-form expressions of objective function σ_i are achieved in this subsection. At the first stage, we focus on single-phase inverters. For a closed-form representation, the following series which can be found in (Hansen, 1975) are used:

$$\beta_4(x)=\sum_{k=1}^{\infty}\frac{\cos[(2k+1)x]}{(2k+1)^4}=\frac{\pi}{96}(\pi-2x)(\pi^2+2\pi x-2x^2),\ 0\le x\le\pi. \tag{6}$$

By introducing an auxiliary function

$$\zeta(\alpha)=\sum_{K\in S_{1\phi}}\frac{v_K^2(\alpha)}{K^2}+V_1^2(\alpha), \tag{7}$$

the objective function σ_i may be written as

$$\sigma_i=\sqrt{\zeta(\alpha)-V_1^2(\alpha)}. \tag{8}$$

Using Eqs.(3) and (6), $\zeta(\alpha)$ can be expanded as follows:

$$\begin{aligned}\zeta(\alpha)&=\frac{16}{\pi^2}\sum_{k=0}^{\infty}\left\{\frac{1}{(2k+1)^4}\left(\sum_{i=0}^{N}h_i\cos[(2k+1)\alpha_i]\right)^2\right\}\\&=\frac{16}{\pi^2}\sum_{k=0}^{\infty}\left\{\frac{1}{(2k+1)^4}\left(\sum_{i=0}^{N}h_i^2\cos^2[(2k+1)\alpha_i]\right.\right.\\&\quad\left.\left.+\sum_{i=0}^{N-1}\sum_{j=i+1}^{N}2h_ih_j\cos[(2k+1)\alpha_i]\cos[(2k+1)\alpha_j]\right)\right\}\\&=\frac{16}{\pi^2}\sum_{i=0}^{N}\frac{h_i^2}{2}\left\{\sum_{k=0}^{\infty}\frac{1}{(2k+1)^4}+\sum_{k=0}^{\infty}\frac{\cos[(2k+1)(2\alpha_i)]}{(2k+1)^4}\right\}\\&\quad+\frac{16}{\pi^2}\sum_{i=0}^{N-1}\left\{h_i\sum_{j=i+1}^{N}h_j\left(\sum_{k=0}^{\infty}\frac{\cos[(2k+1)(\alpha_i+\alpha_j)]}{(2k+1)^4}\right)\right\}\\&\quad+\frac{16}{\pi^2}\sum_{i=0}^{N-1}\left\{h_i\sum_{j=i+1}^{N}h_j\left(\sum_{k=0}^{\infty}\frac{\cos[(2k+1)(\alpha_j-\alpha_i)]}{(2k+1)^4}\right)\right\}.\end{aligned} \tag{9}$$

Then, using Eq.(6), the desired closed-form expression for $\zeta(\alpha)$ is obtained:

$$\begin{aligned}\zeta(\alpha)&=\frac{16}{\pi^2}\left\{\sum_{i=0}^{N}\frac{h_i^2}{2}[\beta_4(0)+\beta_4(2\alpha_i)]\right.\\&\quad\left.+\sum_{i=0}^{N-1}\left(h_i\sum_{j=i+1}^{N}h_j[\beta_4(\alpha_j+\alpha_i)+\beta_4(\alpha_j-\alpha_i)]\right)\right\}.\end{aligned} \tag{10}$$

To derive the closed-form expression for three-phase inverters (the application of interest herein), the triple harmonics should be removed from Eq.(7). Thus, simplification of the following series

$$\sum_{k\in S_t}\left(\frac{V_k(\alpha)}{k}\right)^2, \tag{11}$$

in which S_t={3, 9, 15, …, 6l+3, …}=3{1, 3, 5, …, 2l+1, …}=3$S_{1\phi}$ is necessary. Also noticing that

$$\begin{aligned}V_{3(2k+1)}(\alpha)&=\frac{4}{3(2k+1)\pi}\sum_{i=0}^{N}h_i\cos[3(2k+1)\alpha_i]\\&=\frac{V_{(2k+1)}(3\alpha)}{3},\end{aligned} \tag{12}$$

we have

$$\begin{aligned}\sum_{k\in S_t}\left(\frac{V_k(\alpha)}{k}\right)^2&=\sum_{k=0}^{\infty}\left(\frac{V_{3(2k+1)}(\alpha)}{3(2k+1)}\right)^2\\&=\frac{1}{81}\sum_{k=0}^{\infty}\left(\frac{V_{2k+1}(3\alpha)}{2k+1}\right)^2=\frac{\zeta(3\alpha)}{81}.\end{aligned} \tag{13}$$

Therefore, a closed-form expression is obtained for three-phase inverters as follows:

$$\sigma_i=\sqrt{\zeta(\alpha)-\zeta(3\alpha)/81-V_1^2(\alpha)}. \tag{14}$$

Similar to Eq.(10) which involves functions $\beta_4(2\alpha_i)$ and $\beta_4(\alpha_j+\alpha_i)$, the expression for $\zeta(3\alpha)$ contains functions $\beta_4(6\alpha_i)$ and $\beta_4(3\alpha_j+3\alpha_i)$. As each angle α_i lies in the interval [0, π/2], the values of $6\alpha_i$ and $3\alpha_j+3\alpha_i$ may well exceed the range $0\le x\le\pi$, over which function $\beta_4(x)$ has been defined in Eq.(6). Thus, it is necessary to extend the definition interval of $\beta_4(x)$ from [0, π/2] to [0, 3π]. Noticing that $\cos x=-\cos(x-\pi)$ for x in [0, π/2] and $\cos x=\cos(x-2\pi)$ for $2\pi\le x\le3\pi$ and using Eq.(6), we have

$$\beta_4(x)=\begin{cases}\dfrac{\pi}{96}(\pi-2x)(\pi^2+2\pi x-2x^2), & 0\le x\le\pi,\\[2mm]\dfrac{\pi}{96}(3\pi-2x)(3\pi^2-6\pi x+2x^2), & \pi\le x\le2\pi,\\[2mm]\dfrac{\pi}{96}(2x-5\pi)(11\pi^2-10\pi x+2x^2), & 2\pi\le x\le3\pi.\end{cases} \tag{15}$$

This completes the derivation of the closed-form objective function expression for three-phase inverters.

Output voltage regulation

The fundamental component of PWM is determined by the modulation index (M), which may be

assumed to have any value between 0 and $4/\pi$ for normalized PWM waveform with unit magnitudes. The nominal working point of the system is determined by the modulation index (Holtz, 1992). As such, our purpose is to use the designed system at high modulation indices. During transients, start-up, and changes in speed and load torque, the modulation index is pre-determined by the inverter. Moreover, for higher torque output of the machinery system, the modulation index and number of switching instants are related to each other in a special manner. This point is completely covered in Section 3 of (Sayyh *et al*., 2006b).

Considering the constraint $V_1=M$ and Eq.(4), it can be shown that the Nth switching angle α_N is dependent on modulation index and the rest of $N-1$ switching angles. Hence, one decision variable α_N can be eliminated explicitly,

$$\alpha_N = \arccos\left(\frac{1}{h_N}\left(\frac{M\pi}{4}-\sum_{i=0}^{N-1}h_i\cos\alpha_i\right)\right). \qquad (16)$$

Using Eq.(16) allows the equality constraint ($V_1=M$) to be satisfied automatically in all the solutions used in the optimization process.

OPTIMIZATION PROCEDURE

Generalities

The need for numerical optimization algorithms arises from almost every field of engineering, science, and business. This is because in real world optimization problems, the objective function and its constraints are often not analytically treatable or are even not given in closed-form, e.g., if the function dentition is based on a simulation model (Schwefel, 1979; Bäck *et al*., 1996).

Since nonlinearities and complex interactions among problem variables often exist in real world optimization problems, the search space usually contains local optimal solutions: multimodality. As a numerical algorithm is expected to perform the task of global optimization of the objective function, classical methods usually get attracted to locally optimal solutions when applied. In addition, the possibility of failing to locate the desired global solution increases with the increase of the problem dimensions.

For the scope of this study, local optimal solutions at definite modulation indices M=0.9, 1.0, 1.1, and 1.2 with N=5 are listed in Tables 1~4. Comparisons with global optimum solutions are also made at definite operating points.

Table 1 Local optimal pulse patterns at M=0.9 with N=5, and comparison with global optimal pattern α=(0.180 9, 0.915 3, 1.393 1, 1.480 7) with $\sigma_{i(\mathrm{Global})}$=0.028 09

No.	Pulse pattern	THCD	Error (%)
1	(0.108 1, 0.455 4, 0.554 7, 1.230 0, 1.326 9)	0.031 04	10.48
2	(0.113 9, 1.215 6, 1.289 8, 1.428 7, 1.498 7)	0.028 91	2.91
3	(0.090 9, 0.210 1, 0.381 8, 0.687 6, 0.822 5)	0.038 25	36.13
4	(0.058 3, 0.127 1, 0.176 7, 1.289 0, 1.429 7)	0.037 62	33.91

Table 2 Local optimal pulse patterns at M=1.0 with N=5, and comparison with global optimal pattern α=(0.128 9, 1.255 8, 1.308 1, 1.448 4, 1.497 6) with $\sigma_{i(\mathrm{Global})}$=0.027 60

No.	Pulse pattern	THCD	Error (%)
1	(0.123 1, 0.464 3, 0.535 3, 1.268 7, 1.336 9)	0.028 41	2.93
2	(0.169 3, 0.934 3, 0.966 8, 1.404 2, 1.471 4)	0.028 01	1.47
3	(0.068 0, 0.152 9, 0.208 0, 1.333 7, 1.430 6)	0.029 50	6.89
4	(0.098 9, 0.237 8, 0.371 2, 0.694 3, 0.786 9)	0.031 26	13.26

Table 3 Local optimal pulse patterns at M=1.1 with N=5, and comparison with global optimal pattern α=(0.078 8, 0.184 0, 0.243 7, 1.397 1, 1.449 9) with $\sigma_{i(\mathrm{Global})}$=0.019 81

No.	Pulse pattern	THCD	Error (%)
1	(0.158 2, 0.954 8, 0.967 1, 1.418 4, 1.464 3)	0.028 34	43.11
2	(0.117 6, 0.362 3, 0.409 4, 1.299 2, 1.344 0)	0.024 06	21.47
3	(0.105 7, 0.265 1, 0.360 9, 0.697 8, 0.747 6)	0.023 67	19.48
4	(0.143 1, 1.316 7, 1.346 8, 1.475 2, 1.503 8)	0.027 10	36.85

Table 4 Local optimal pulse patterns at M=1.2 with N=5, and comparison with global optimal pattern α=(0.074 6, 0.175 4, 0.231 2, 0.385 7, 0.423 1) with $\sigma_{i(\mathrm{Global})}$=0.015 32

No.	Pulse pattern	THCD	Error (%)
1	(0.087 2, 0.212 6, 0.274 1, 1.514 5, 1.524 7)	0.017 07	11.38
2	(0.153 7, 1.008 6, 1.008 7, 1.476 9, 1.493 9)	0.030 51	99.10
3	(0.100 9, 0.261 1, 0.321 1, 1.273 1, 1.279 8)	0.020 50	33.82
4	(0.153 7, 0.837 5, 0.837 6, 1.476 9, 1.493 9)	0.030 51	99.10

These local optimal solutions are the ones that conventional optimization algorithms are prone to get trapped in. The value of σ_i in each case is calculated by plugging the local optimal pulse patterns in Eq.(14), which provides an explicit formula for calculating THCD. Moreover, the GA optimization technique is also used to accomplish the global optimum solution. By comparison between error percentages $(=(\sigma_{i(\text{Local})}-\sigma_{i(\text{Global})})/\sigma_{i(\text{Global})}\times 100\%)$, particularly at higher modulation indices, using a developed optimization technique to find the global optimum solution to avoid unwanted distortions seems completely justifiable.

As observed in these tables, the error percentage values are high in most cases. As mentioned earlier, minimization of motor harmonic current distortion also corresponds to the minimization of harmonic copper losses of the motor windings. Losses in the machine should be considered at least for the following reasons (Fitzgerald *et al.*, 1985): (1) Losses determine the efficiency of the machine and appreciably influence its operating cost; (2) Losses determine the heating of the machine and hence the rating or power output that can be determined without undue deterioration of the insulation.

Additionally, it can be investigated that local optimal solutions increase dramatically with the increase of decision variables. The arguments above along with the high power level of operation (typically several megawatts) convince us to concentrate all of our efforts to find the global optimum solution.

Genetic algorithm approach

Over the last decade, genetic algorithms (GAs) (Golberg, 1989; Davis, 1991; Deb, 2001) have been extensively used as a search and optimization tool in dealing with difficult global optimization problems (Bäck *et al.*, 1997; Sayyah *et al.*, 2006 a). The primary reasons for their success lie in the gain of flexibility and adaptability to the task at hand, in combination with robust performance (although this depends on the problem class) and global search characteristics. They are rooted in the concepts of natural selection and survival of the fittest. Although GAs are often viewed as function optimizers, the range of problems to which GAs have been applied is quite broad. A GA starts with a population of randomly generated chromosomes. One then evaluates these structures and allocates reproductive opportunities in a way that those chromosomes representing a better solution to the target problem are given more chances to 'reproduce'. This procedure is repeated through a number of generations to approach the global optimum solution (the best).

In the problem discussed herein, our aim is to choose $N-1$ switching instants in an electrical cycle (Fig.1) for turning switches on and off in a full bridge inverter to produce the desired fundamental amplitude while optimizing the defined objective functions.

Optimization methodology

The GA methodology structure for the problem considered herein is as follows:

(1) Representation. Parameter representation or encoding is a process of representing the model parameter values in GA, so that the computer can interact with these values. Among various types of parameter coding methods, bit string coding (used in this study) and real-valued coding are the most frequently ones.

(2) Population size and initialization. Population size is the number of chromosomes presented in a population. Larger population sizes increase the amount of variation presented in the population (or population diversity), but at the expense of requiring more function evaluations (Goldberg, 1989). On the other hand, a small population size can cause GA to converge prematurely to a suboptimal solution. It should be pointed out that the population size is both application dependent and related to the length of the chromosome (i.e., string length).

An initial population of individuals is chosen. An $m\times(N-1)$ random matrix is generated. The first and second dimensions of the matrix represent the number of individuals (population size) and the number of decision variables that lie in $[0, \pi/2]$, respectively. The rows of the matrix are sorted in ascending order to satisfy Eq.(1). This makes all solutions feasible for undergoing next steps in the procedure. Population sizes for the two cases of three and five switching angles are considered 20 and 60, respectively, to yield satisfactory results.

(3) Evaluation. The major component of GA is its evaluation function, which serves as a major link between the algorithm and the problem being solved.

The evaluation function is used to distinguish between better and worse individuals in the population. Hence it provides an important feedback for the search process. Objective function values of all members in the population are evaluated by the objective function defined in Eq.(14).

(4) Selection. The selection process determines which chromosomes participate in reproduction to generate the next population (in the next generation) according to their objective function values in the current population. In general, this process takes advantage of the fittest solutions by giving them greater weights when selecting the next generation and hence leads to better solutions to the problem. This study utilizes Roulette-wheel selection (Mitchell, 1996), which is an easy-to-implement and commonly-used method for selection mechanism.

(5) Recombination. In this step, members of the population undergo transformations by genetic operators to form the next generation. These operators include 'crossover' and 'mutation'. The crossover operator is used to create new chromosomes for the next generation by randomly combining two selected chromosomes from the current generation through the selection process, and takes place according to a given probability P_c.

Mutation introduces innovation into the population by randomly modifying the chromosomes. It prevents the population from becoming saturated with chromosomes that are all similar, and reduces the chance of premature convergence. The parameter P_m determines the probability that mutation will occur. In this study, the selected values for P_c and P_m are 0.85 and 0.05, respectively.

(6) Elitism. At each iteration of GA, it is convenient to identify the best individuals, which are always transferred to the next generation. This so-called 'elitist strategy' guarantees against the loss of good information embedded in the best individual produced thus far. The number of elite counts considered here is 5% of the population size.

(7) Termination criteria. The algorithm is repeated until a termination criterion is reached. Termination criteria are defined relating to the nature of the problem. The termination criterion in this study is the maximum number of generations, which is set to 500.

MINIMIZATION OF THCD

Three switching angles

In this case, the aim of optimization is to find a set of solutions (α_1, α_2) that minimizes the objective function, Eq.(14). The third switching angle also follows Eq.(16). Fig.3 shows the α_1, α_2 and α_3 vs modulation index that varies from 0 to M_{max}. A step change in the trajectory of switching angles occurs in M=1.17, due to alteration of the global optimal solution. The variation of each angle is fairly linear in subintervals of $M\in[0, 1]$ and $M\in[1.175, 1.215]$. The THCD of the waveform as defined by Eq.(14) is illustrated in Fig.4. Quantitative comparisons between harmonic elimination method and minimization of harmonic current distortion are also given in Fig.4. Set 1 and Set 2 shown in Fig.4 correspond to THCD of the two sets of solutions that have been accomplished for the elimination of the 5th and 7th harmonics in the case of three switching angles in (Chiasson, 2004), respectively. As Fig.4 shows, minimization of harmonic current distortion results in reduction of about 6.1% and 45.11% relative to Set 1 and Set 2, respectively.

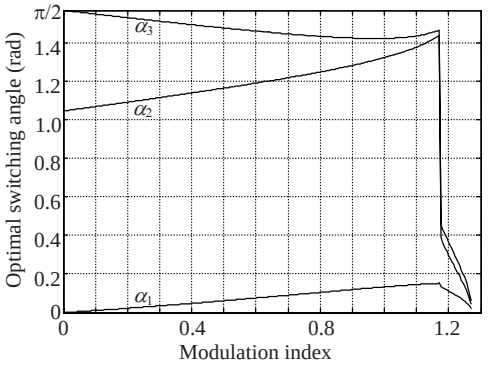

Fig.3 Optimal switching angles (N=3)

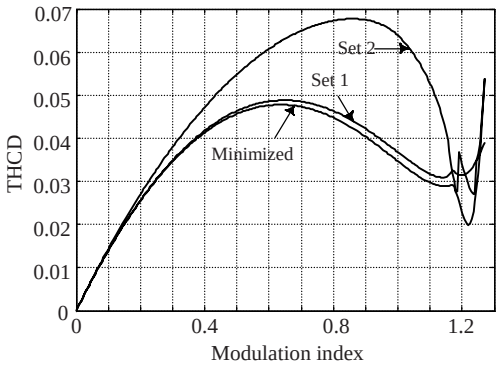

Fig.4 Minimized total harmonic current distortion (THCD) and THCD of harmonic elimination equations (N=3)

Fig.5 shows the voltage harmonic content magnitude vs modulation index and harmonic number.

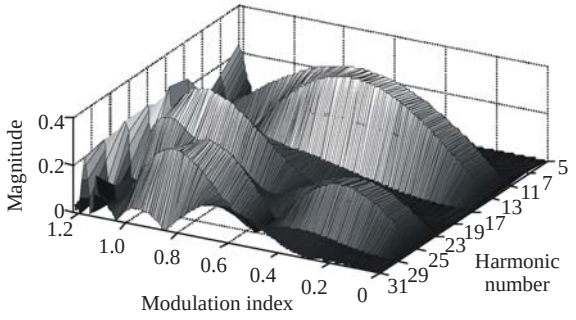

Fig.5 Harmonic content magnitude vs modulation index and harmonic number (*N*=3)

Five switching angles

Like in the case of three switching angles, the goal is to minimize the THCD by determination of optimal solution (α_1, α_2, α_3, α_4). Optimal switching angles vs modulation index are illustrated in Fig.6.

As observed in Fig.6, three step changes occur in the trajectory of switches due to alteration in global optimum solution. While most of the point-to-point optimization algorithms would fail in locating the global optimum solution due to the fact that calculation of the current optimal point in these algorithms is dependent on the information of its preceding point(s), GA has the feature of incorporating a stochastic-based process into the search procedure to find the global optimal point. This point mostly arises with the increase of decision variables or complexity of the objective function (present work).

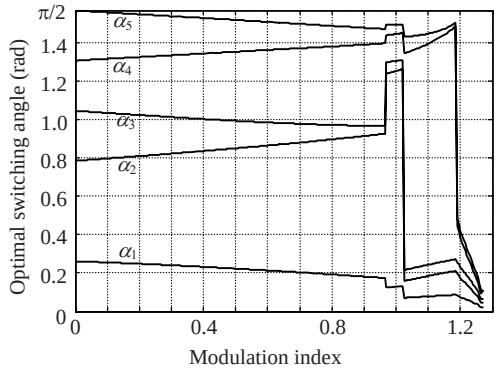

Fig.6 Optimal switching angles (*N*=5)

It should be stated that in some situations, to achieve the global optimal solution, we used a trial-and-error process, due to the presence of many local optimal solutions. With a good precision, it can be observed that in all four subintervals of the modulation index (i.e., [0, 0.970], [0.975, 1.015], [1.020, 1.180] and [1.185, 1.270]), the switching trajectories can be approximated to a straight line. In practical situations, the calculated switching angles are stored in read-only memory (ROM) and served as a look-up table. During real-time operation, the required fundamental amplitude is used for addressing the corresponding switching angles in the look-up table and read out for controlling the inverter. To avoid the use of large memory components and to improve the flexibility and maintenance of the system, a real-time production of switching instants can be performed from simple functions that approximate on-line calculated solution trajectories (Sun *et al.*, 1996). The accuracy of the on-line generated switching instants has a great reliance on the proximity of functions and could be increased, at least theoretically, to any extent by using high-order polynomials. The corresponding THCD of the optimized waveform is illustrated in Fig.7.

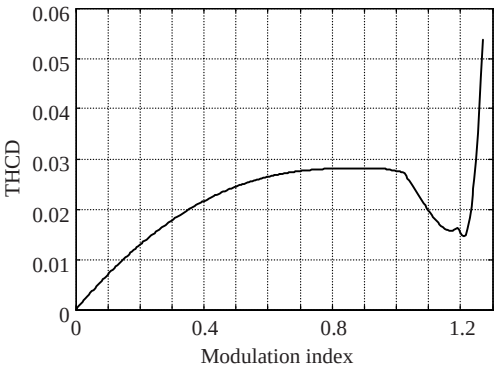

Fig.7 Minimized total harmonic current distortion (THCD) (*N*=5)

An optimized PWM waveform modulated at *M*=0.9 with *N*=5 is illustrated in Fig.8. The five optimized switching angles in the first quarter period are α_1=0.180 7, α_2=0.915 3, α_3=0.969 0, α_4=1.393 1, and α_5=1.480 7. Now, we consider the inverter-fed induction motor system depicted in Fig.9, in which GTOs are used as power semiconductor devices. However, GTOs must normally be used with snubbers (not shown in this figure), and thus any realistic description of the GTO switching behavior must include the effects of the snubber circuits.

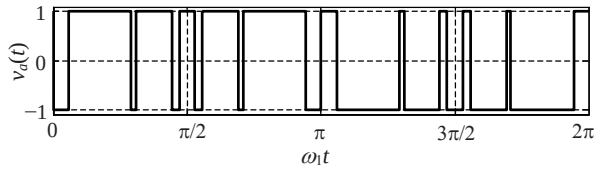

Fig.8 Optimized $v_a(t)$ waveform modulated at M=0.9 (N=5)

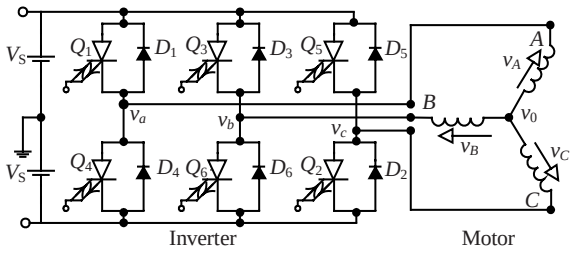

Fig.9 A three-phase inverter feeding an induction motor

It is important to realize that GTOs are only used in medium to high power applications (like the conditions considered herein), where the voltage and current levels are large, and the other solid-state components that may be used in conjunction with the GTOs are likely to be rather slow (Mohan *et al.*, 1995).

Suppose one LN (line to neutral) inverter output voltage $v_a(t)$ resembles this optimized waveform. Then $v_b(t)$ and $v_c(t)$ are obtained as

$$v_b(t)=v_a\left(t-\frac{2\pi}{3\omega_1}\right),\quad v_c(t)=v_a\left(t-\frac{4\pi}{3\omega_1}\right),\qquad(17)$$

where ω_1 is the fundamental angular frequency of the inverter output.

In this case, LL (line to line) voltages at the load side are $v_{AB}(t)=v_a(t)-v_b(t)$, $v_{BC}(t)=v_b(t)-v_c(t)$, and $v_{CA}(t)=v_c(t)-v_a(t)$. As the three windings are symmetrical, the neutral voltage $v_0(t)$ is

$$v_0(t)=\left(v_a(t)+v_b(t)+v_c(t)\right)/3.\qquad(18)$$

The waveform of phase voltage $v_A(t)$ is illustrated in Fig.10c.

Using the transformation below,

$$\begin{pmatrix}v_\alpha(t)\\ v_\beta(t)\end{pmatrix}=\frac{2}{3}\begin{pmatrix}1 & -\frac{1}{2} & -\frac{1}{2}\\ 0 & \frac{\sqrt{3}}{2} & -\frac{\sqrt{3}}{2}\end{pmatrix}\begin{pmatrix}v_A(t)\\ v_B(t)\\ v_C(t)\end{pmatrix},\qquad(19)$$

the three symmetrical phase voltages $v_A(t)$, $v_B(t)$, and $v_C(t)$ can be transformed into α-β coordinates. Furthermore, motor currents $i_\alpha(t)$ and $i_\beta(t)$ in this coordinate system are proportional to the integrals of the voltages $v_\alpha(t)$ and $v_\beta(t)$, respectively, assuming that motor resistances are negligible. The voltage and current waveforms in the α-β coordinate system are illustrated in Figs.10d and 10e, respectively.

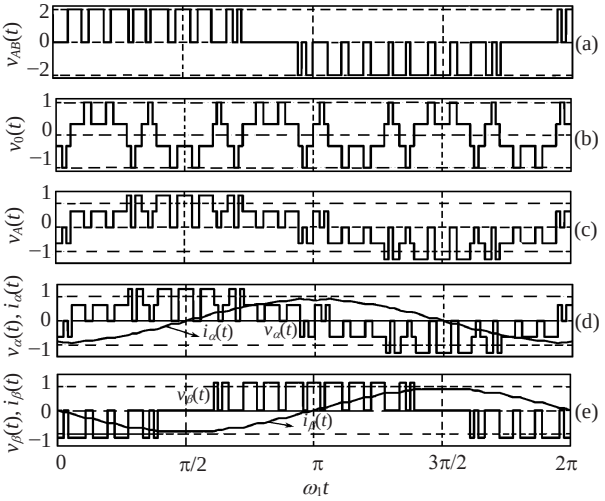

Fig.10 Waveforms in an inverter-fed induction motor system shown in Fig.9. (a) $v_{AB}(t)$; (b) $v_0(t)$; (c) $v_A(t)$; (d) $v_\alpha(t)$ and $i_\alpha(t)$; (e) $v_\beta(t)$ and $i_\beta(t)$

Since motor fluxes $\phi_\alpha(t)$ and $\phi_\beta(t)$ in α-β coordinates are proportional to $i_\alpha(t)$ and $i_\beta(t)$, respectively, the trajectory of $i_\alpha(t)$−$i_\beta(t)$ in a complex plane represents the trajectory of motor fluxes. This is shown in Fig.11.

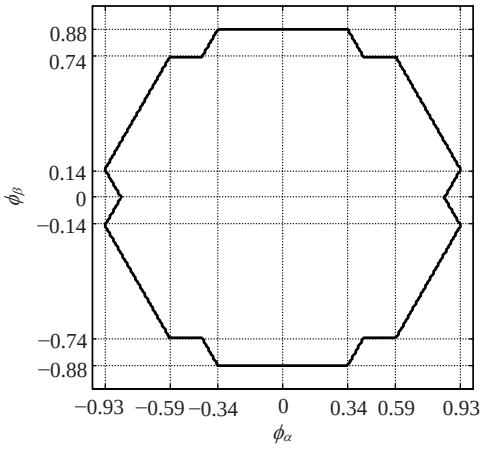

Fig.11 Trajectory of motor flux

TORQUE PULSATION REDUCTION AND OPTIMIZATION OF THCD

Pulsating torques are produced by the interaction of air gap flux and rotor MMF waves of different orders. The pulsating torque, which is mainly affected by the presence of low-order harmonics, tends to cause jitter in the machine speed, while the effect of high-frequency components will be smoothened due to system mechanical inertia. The speed jitter may be aggravated if the pulsing frequency is low, or if the system mechanical inertia is small. The pulsing torque frequency may be near the mechanical resonance of the drive system, and this may result in severe shaft vibration, causing fatigue, wearing of gear teeth, and unsatisfactory performance in the feedback control system.

Based on the discussion above, our aim in this section is to limit the 5th, 7th, 11th, and 13th harmonic currents (in the case of N=5) while THCD is minimized, in order to reduce the torque pulsation. Fig.12 shows these harmonics using the optimal pulse patterns accomplished in the previous section. Four inequality constraints have been realized in each limitation value, λ. They are

$$I_h \le \lambda, \tag{20}$$

in which h=5, 7, 11, 13. These constraints should be handled in the optimization procedure.

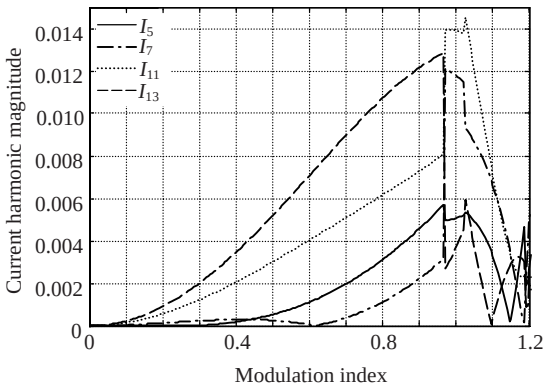

Fig.12 Current harmonics vs modulation index (N=5)

A vast majority of industrial engineering optimization problems (like in this case) are constrained problems. The presence of constraints significantly impacts the performance of every optimization algorithm (Michalewicz *et al.*, 1996). Generally, evolutionary computation techniques appear particularly apt for addressing constrained optimization problems. Classic linear and nonlinear programming methods are often either unsuitable or empirical when applied to constrained optimization problems which present the difficulties of potentially nonconvex or even disjoint feasible regions (Kim and Myung, 1997). Difficulties arise because either the amount of computation required quickly becomes unmanageable as the size of the problem increases, or the constraints violate the required assumptions, such as differentiability or convexity. In this problem, the set of constraints in Eq.(20) is handled using the penalty function method, which is the most common approach in the GAs. It requires only the straightforward modification of the evaluation function *eval* as follows:

$$eval(\alpha) = f(\alpha) + W \cdot penalty(\alpha), \tag{21}$$

where f is the objective function, and $penalty(\alpha)$ is zero if no violation occurs, and positive otherwise (for minimization problems). Usually, the *penalty* function is based on the distance of a solution from the feasible region, or on the effect to repair the solution, i.e., to force into the feasible region. W is the user-defined weight, prescribing how severely constraint violations are weighted. Considering Fig.12, in the subintervals of modulation index, where $I_h \le \lambda$, the optimization results are the same as obtained in the case of minimizing the THCD.

Fig.13 shows the optimal pulse patterns in the case of λ=0.01. As in the case of minimizing the THCD, step changes occur in trajectory of optimal solutions in certain modulation indices due to alteration of global optimal solution. The normalized FFTs of the optimized voltage waveforms (with respect to the fundamental), modulated at M=0.9 in three cases of minimized THCD, λ=0.01, and λ=0.008 are shown in Fig.14 (current harmonics can be achieved using Eq.(4)). The total energy of harmonics in a PWM waveform is constant, depending only on the fundamental amplitude (Sun, 1995), regardless of the actual waveform structure. Optimizing the waveform should not be considered as elimination or reduction of the total energy, but to alter its distribution among different frequency components. Noticing this fact, the

increase in the THCD in the case of λ=0.008 with regard to minimized THCD in the subinterval of $M\in$[0.65, 1.09] is justifiable (Fig.15). That is, suppression of chosen harmonics leads to increase in the value of THCD. These results can be generalized by decreasing the limitation value, λ, and running the optimization program, to obtain new optimal results.

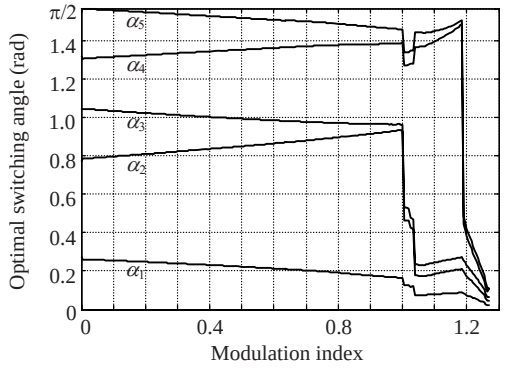

Fig.13 Optimal pulse patterns in the case of λ=0.01

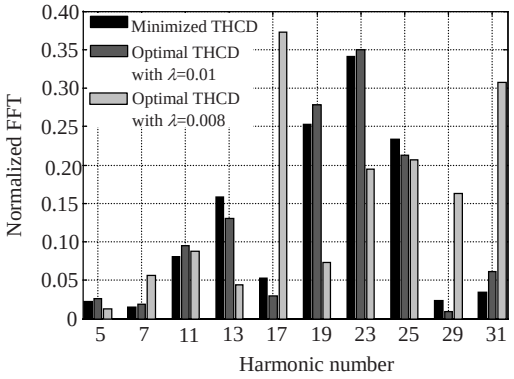

Fig.14 Normalized FFT (with respect to the fundamental voltage component) vs harmonic number at M=0.9

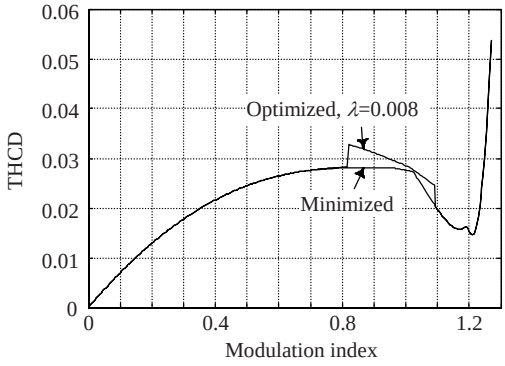

Fig.15 Comparison of minimized and optimized total harmonic current distortion (THCD) in the case of λ=0.008

CONCLUSION

Optimal pulse patterns to the problem of minimization of THCD in high-power (typically several megawatts) induction motors were presented for the two cases of three and five switching angles. The GA optimization technique was applied. Its distinguished advantages over the deterministic optimization methods lie in that it possesses the ability to span the search space with more likelihood of finding the global optimum solution particularly when decision variables increase. Furthermore, it does not require derivative information and is distinctively apt for addressing constrained optimization problems. The benefits of optimization are remarkable, considering the total power of the system.

Torque pulsation is mainly affected by the presence of low-order frequency harmonic components. Pulsing torques can cause troublesome speed fluctuations and shaft vibration. In this study, we constrained the 5th, 7th, 11th, and 13th current harmonics to some pre-specified values to mitigate the detrimental effects of these harmonics (in the case of five switching angles). At the same time, the THCD was optimized while maintaining the required fundamental output voltage. New optimal pulse patterns yielded. It is intuitively obvious that this optimization can be resumed to accomplish new optimal results.

References

Asumadu, J.A., Hoft, R.G., 1989. Microprocessor-based sinusoidal waveform synthesis using Walsh and related orthogonal functions. *IEEE Trans. on Power Electron.*, **4**(2):234-241. [doi:10.1109/63.24908]

Bäck, T., Hammel, U., Schäutz, M., Schwefel, H.P., Sprave, J., 1996. Applications of Evolutionary Algorithms at the Center for Applied Systems Analysis. *In:* Desideri, J.A., Hirsch, C., le Tallec, P., *et al.* (Eds.), Computational Methods in Applied Sciences. Wiley, Chichester, UK, p.243-250.

Bäck, T., Hammel, U., Schwefel, H.P., 1997. Evolutionary computation: comments on the history and current state. *IEEE Trans. on Evol. Comput.*, **1**(1):3-17. [doi:10.1109/4235.585888]

Bose, B.K., 1986. Power Electronics and AC Drives. Prentice-Hall, NJ.

Chen, C., 1999. Linear Systems Theory and Design (3rd Ed.). Oxford University Press, London, UK.

Chiasson, J.N., Tolbert, L.M., McKenzie, K., Du, Z., 2002. Eliminating Harmonics in a Multilevel Converter Using

Resultant Theory. IEEE Power Electronics Specialists Conf., Cairns, Australia, p.503-508.

Chiasson, J.N., Tolbert, L.M., McKenzie, K., Du, Z., 2004. A complete solution to the harmonic elimination problem. *IEEE Trans. on Power Electron.*, **19**(2):491-499. [doi:10.1109/TPEL.2003.823207]

Cox, D., Little, J., OShea, D., 1996. Ideals, Varieties, and Algorithms: An Introduction to Computational Algebraic Geometry and Commutative Algebra (2nd Ed.). Springer-Verlag, NY.

Davis, L., 1991. Handbook of Genetic Algorithms. van Nostrand Reinhold, New York.

Deb, K., 2001. Multi-objective Optimization Using Evolutionary Algorithms. Wiley, Chichester, UK.

Fitzgerald, A.E., Kingsley, C., Umans, S.D., 1985. Electric Machinery (4th Ed.). McGraw Hill, New York, NY.

Goldberg, D., 1989. Genetic Algorithms in Search, Optimization, and Machine Learning. Reading, Addison-Wesley, MA.

Hansen, E.R., 1975. A Table of Series and Products. Prentice-Hall, Englewood Cliffs, NJ.

Holtz, J., 1992. Pulsewidth modulation—a survey. *IEEE Trans. on Ind. Electron.*, **39**(5):410-420. [doi:10.1109/41.161472]

Kailath, T., 1980. Linear Systems. Englewood Cliffs, Prentice-Hall, NJ.

Kim, J.H., Myung, H., 1997. Evolutionary programming techniques for constrained optimization problems. *IEEE Trans. on Evol. Comput.*, **1**(2):129-140. [doi:10.1109/4235.687880]

Michalewicz, Z., Dasgupta, D., le Riche, R.G., Schoenauer, M., 1996. Evolutionary algorithms for constrained engineering problems. *Comput. Ind. Eng. J.*, **30**(4):851-870. [doi:10.1016/0360-8352(96)00037-X]

Mitchell, M., 1996. An Introduction to Genetic Algorithms (1st Ed.). Prentice-Hall, India.

Mohan, N., Undeland, T.M., Robbins, W.P., 1995. Power Electronics: Converters, Applications, and Design (2nd Ed.). Wiley, New York.

Murphy, J.M.D., Turnbull, F.G., 1988. Power Electronic Control of AC Motors. Pergamon Press, Oxford.

Ozpineci, B., Tolbert, L.M., Chiasson, J.N., 2005. Harmonic optimization of multilevel converters using genetic algorithms. *IEEE Power Electron. Lett.*, **3**(3):92-95. [doi:10.1109/LPEL.2005.856713]

Park, M.H., Ahn, D.S., Won, C.Y., Lee, H.K., Kim, T.H., 1990. Microprocessor-based new Harmonic Elimination Method Using Walsh-Fourier Transformation. Proc. Int. Power Electron. Conf., p.799-808.

Rezazadeh, A.R., Sayyah, A., Aflaki, M., 2006. Modulation Error Observation and Regulation for Use in On-line Optimal PWM Fed High Power Synchronous Motors. Proc. 1st IEEE Conf. on Industrial Electronics and Applications, Singapore, p.1300-1307.

Sathyanarayan, S.R., Birru, H.K., Chellapilla, K., 1999. Evolving Nonlinear Time-series Models Using Evolutionary Programming. Proc. Congress Evolutionary Computation, **1**:236-243.

Sayyah, A., Aflaki, M., Rezazade, A.R., 2006a. Optimal PWM for Minimization of Total Harmonic Current Distortion in High-power Induction Motors Using Genetic Algorithms. Proc. IEEE Int. Conf. SICE-ICCAS, Busan, Korea, p.5494-5499.

Sayyah, A., Aflaki, M., Rezazade, A.R., 2006b. Optimization of THD and Suppressing Certain Order Harmonics in PWM Inverters Using Genetic Algorithms. Proc. IEEE Int. Symp. Intelligent control, Munich, Germany, p.874-879.

Schwefel, H.P., 1979. Direct Search for Optimal Parameters Within Simulation Models. Proc. 12th Annual Simulation Symp., Tampa, FL, p.91-102.

Sun, J., 1995. Optimal Pulse Width Modulation Techniques for High-power Voltage-source Inverters. PhD Thesis, VDI VERLAG, Däusseldorf.

Sun, J., Grotstollen, H., 1994. Pulse Width Modulation Based on Real-time Solution of Algebraic Harmonic Elimination Equations. Proc. 20th Int. Conf. on Industrial Electronics, Control and Instrumentation, **1**:79-84.

Sun, J., Beineke, S., Grotstollen, H., 1996. Optimal PWM based on real-time solution of harmonic elimination equations. *IEEE Trans. on Power Electron.*, **11**(4):612-621. [doi:10.1109/63.506127]